

Electronic properties of CeIn₃ under high pressure near the quantum critical point

G. Knebel, D. Braithwaite, P. C. Canfield,* G. Lapertot, and J. Flouquet

Département de Recherche Fondamentale sur la Matière Condensée, SPSMS, CEA Grenoble, 38054 Grenoble, France

(Received 24 November 2000; revised manuscript received 9 March 2001; published 19 December 2001)

We present a detailed study of the phase diagram of the antiferromagnetic Kondo-lattice compound CeIn₃ under pressure up to 100 kbar by resistivity measurements. Antiferromagnetic order vanishes at a critical pressure $P_c = 26.5$ kbar. At this quantum critical point a complete superconducting transition is found in the pressure range from 24 to 27 kbar. Normal state properties near the critical point show strong deviations from Fermi-liquid behavior. In magnetic fields just above the upper critical field Fermi-liquid behavior is restored. For $P > P_c$, $\rho(T)$ shows a clean T^2 dependence up to a crossover temperature T_I which increases linearly with pressure. The temperature dependence of the upper critical field H_{c2} can be described with a strong coupling model in the clean limit.

DOI: 10.1103/PhysRevB.65.024425

PACS number(s): 71.27.+a, 71.10.Hf, 74.70.Tx

I. INTRODUCTION

The application of external pressure is an excellent tool to vary the ground state properties of intermetallic Ce heavy-fermion compounds, which are located just in the vicinity of a magnetic instability. The ground state is determined by the competition of the Ruderman-Kittel interaction, which leads to a long range magnetically ordered state, and the Kondo interaction, which results in a screening of the $4f$ moment by the conduction electrons. With this experimental technique the hybridization of the $4f$ electrons and the conduction electrons can be varied in order to study in detail the vanishing of magnetic order at a quantum critical point (QCP). In several Ce compounds a low temperature superconducting phase is found just at a QCP. The pairing mechanism of this unconventional superconductivity may be due to a magnetic interaction.¹ The normal state properties at the magnetic instability usually show a deviation from Fermi-liquid behavior due to the existence of an extended temperature crossover domain down to $T \rightarrow 0$ K at the critical pressure P_c .

CeCu₂Si₂ is the first Ce-based heavy-fermion system showing superconductivity at ambient pressure and seems to be located just at the borderline of an antiferromagnetic ordered state.^{2,3} In a H - T phase diagram the superconducting phase is embedded in a magnetic phase "A," which disappears at $T_A \approx T_c$. The superconducting phase in CeCu₂Si₂ exists over a very broad pressure regime up to 80 kbar and the maximum transition temperature is found at $P \approx 30$ kbar, far away from the magnetic ordered state. Traces of superconductivity have also been found in the nonmagnetic heavy-fermion compound CeNi₂Ge₂ at ambient pressure and above 15 kbar.⁴⁻⁷ Recently superconductivity has been discovered in the new quasi-two-dimensional heavy-fermion systems, CeCoIn₅, with high $T_c = 2.3$ K and CeIrIn₅ ($T_c = 380$ mK).⁸

However, in these systems it is not possible to study the magnetic side of a QCP because although the magnetically ordered state can be induced by doping experiments, these always create defects in the systems which destroy the superconductivity. Recently a superconducting transition has been found in several Ce compounds under hydrostatic pressure just at the border of magnetism where $T_N \rightarrow 0$, notably

in CeCu₂Ge₂,⁹ CeRh₂Si₂,¹⁰ CePd₂Si₂,^{1,11-13} CeIn₃,^{1,14} and very recently CeRhIn₅.¹⁵ All these systems are antiferromagnetically ordered at ambient pressure.

CeIn₃ is an ideal system to study the electronic properties at a QCP. It crystallizes in a simple cubic Cu₃Au structure and is thus less sensitive to small pressure gradients in a pressure cell, which lead to additional uniaxial stress on the sample. At ambient pressure, CeIn₃ orders at $T_N = 10.1$ K in a simple type II antiferromagnetic structure. The Ce moments are aligned antiferromagnetically in adjacent (111) ferromagnetic planes. The ordered magnetic moment of $0.5\mu_B$ is somewhat reduced by comparison with the saturation moment of the Γ_7 doublet, $0.71\mu_B$,^{16,17} which is the ground level for $J = 5/2$ in a cubic crystal field. The crystal field splitting between the low lying doublet and the Γ_8 quartet is of the order 100–200 K.¹⁶⁻¹⁹ The magnetic transition at ambient pressure looks mean-field like.¹⁶

The phase diagram of CeIn₃ was studied under pressure up to 30 kbar.^{1,14,20-22} Neutron scattering experiments show no change in the magnetic structure up to 10 kbar.²¹ With increasing pressure, the Néel temperature T_N decreases first smoothly ($P < 10$ kbar) and then more drastically; it collapses at a critical pressure $P_c \approx 26$ kbar. A superconducting transition was found below 200 mK in the pressure range between 22 and 28 kbar, with the maximum near the QCP.^{1,14}

The aim of this work was to investigate by resistivity measurements the phase diagram CeIn₃ again in order to test its reproducibility near P_c , to extend the measurement far above P_c , and finally to report new features like a careful study of the magnetic anomalies at T_N and the upper superconducting critical field $H_{c2}(T)$.

We give a detailed discussion of the broadening of the resistivity anomaly at T_N near the critical pressure P_c . The temperature dependence of the resistivity in the critical pressure region is also studied for different external magnetic fields. We further extended the pressure range up to 100 kbar to study the recovery of Fermi-liquid behavior on the paramagnetic side of the QCP. In our study we investigated samples grown in a very different way and used somewhat different pressure cells in comparison to earlier work. However, the obtained P - T phase diagram is remarkably similar.

This shows that this kind of phase diagram is robust and reproducible. Finally we present the first study of the upper critical field H_{c2} , to characterize the superconducting phase in more detail to get some information on the microscopic origin of the superconductivity near the QCP.

II. EXPERIMENTAL DETAILS

Single crystals of CeIn_3 were grown out of excess In. By slowly cooling the melt crystals with masses as large as several grams could be grown.²³ Several crystals have been tested to select the sample for the pressure experiment. The resistivity ratio $\rho(300\text{ K})/\rho(4.2\text{ K})$ of the highest quality crystals was about 35. From this crystal a small sample of $600\ \mu\text{m} \times 180\ \mu\text{m} \times 60\ \mu\text{m}$ was prepared. At ambient pressure there was no sign of filamentary superconductivity of In. The measurements under pressure were performed in a Bridgman type cell with nonmagnetic tungsten carbide anvils using steatite as pressure transmitting medium. The pressure was measured by the superconducting transition of Pb. The width of the transition was about 30 mK for pressures lower than 30 kbar. This corresponds to a maximal pressure gradient of less than 1 kbar in this pressure regime. For higher pressures the gradient was slightly higher. The resistivity was measured with a four point lock-in technique at a frequency of 11.7 Hz. The maximal current used was $100\ \mu\text{A}$. The measurements were performed in a conventional ^4He cryostat and in a dilution refrigerator down to 40 mK. In the dilution refrigerator it was possible to measure in magnetic fields up to 6 T. To determine the upper critical field, both field and temperature sweeps were performed. The superconducting transition temperature was always determined by a tangent criterion which is similar to the onset of the transition.

III. RESULTS AND DISCUSSION

In Fig. 1 we summarize the pressure–temperature phase diagram of CeIn_3 . This phase diagram is determined only by resistivity measurements. In addition to the transition temperatures determined in this work, we plotted the pressure dependence of T_N after Ref. 22 (\times) and $T_N(P)$ (\circ) and $T_c(P)$ (\diamond) after Ref. 1. The main results are as follows. (i) With increasing pressure the antiferromagnetic ordering temperature is shifted monotonously to $T_N=0\text{ K}$ for $P_c \approx 26.5 \pm 1\text{ kbar}$. (ii) Around this critical pressure a superconducting phase is found at very low temperatures. (iii) The temperature dependence of the normal state resistivity shows in the critical region strong deviations from Fermi-liquid behavior. (iv) But for pressures $P > P_c$ a Fermi-liquid ground state is recovered below a crossover temperature T_I .

The small differences of the pressure dependence of T_N and T_c of the different experiments are probably due to differences in sample preparation and to the fact that different kinds of pressure cells with different pressure transmitting media have been used. The Cambridge group used a piston-cylinder cell filled with an equal mixture of *iso*-pentane and *n*-pentane. The pressure gradients in this type of cell seem to be lower than in the Bridgman-type cells with steatite as

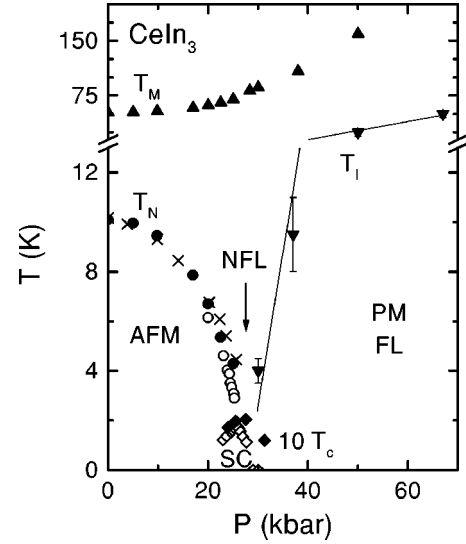


FIG. 1. Phase diagram of CeIn_3 . T_M indicates the temperature of the maximum of the resistivity, T_N the Néel temperature, and T_I the crossover temperature to the Fermi-liquid regime. The superconducting transition temperature T_c is scaled by a factor 10. (\times) after Ref. 22, (\circ) and (\diamond) after Ref. 1.

pressure transmitting medium. In the case of the tetragonal system CePd_2Si_2 the pressure dependence of T_N and T_c is very sensitive to pressure inhomogeneities. The results obtained in a Bridgman-type cell with a solid pressure transmitting medium^{12,13} are different from results obtained on samples of the same platelet in piston cylinder²⁴ or diamond anvil cells,²⁵ and the pressure range where a superconducting transition is found is much broader in the Bridgman study. However, as CeIn_3 is a cubic system, the choice of the pressure cell is not as important as in systems with a lower crystal symmetry and only slight differences are found for the phase diagram obtained by different pressure techniques.

In the following we will discuss the phase diagram in more detail. Figure 2 shows the temperature dependence of the resistivity for selected pressures. As can be seen in the upper frame of Fig. 2 the resistivity at low pressures shows a logarithmic increase between 200 and 70 K. At zero pressure a broad maximum occurs at $T_M \approx 50\text{ K}$. The maximum in the resistivity is probably due to crystal-field effects. For cerium Kondo lattices with rather high Kondo temperatures T_K only one maximum in the resistivity is expected.²⁶ The Kondo temperature of CeIn_3 can be estimated $T_K \approx 10\text{ K}$.²⁷ The first neutron scattering experiments failed to observe resolved crystal-field transitions, however Murani *et al.*¹⁹ determined broad but well-defined crystal-field excitations at $11.6 \pm 0.3\text{ meV}$ with a width of $3 \pm 0.2\text{ meV}$.

At low temperatures the resistivity at zero pressure shows a sharp change in slope at $T_N=10.1\text{ K}$ due to the onset of antiferromagnetic order (Fig. 2 lower frame). In magnetically ordered Kondo-lattice compounds the resistivity can be described by $\rho(T) = \rho_0 + AT^2 + \rho_{mag}(T)$. Here ρ_0 is the temperature independent residual resistivity, the second term corresponds to the scattering between heavy quasiparticles, and the third term to magnon scattering, which depends essentially on the form of the magnon spectrum, which is not

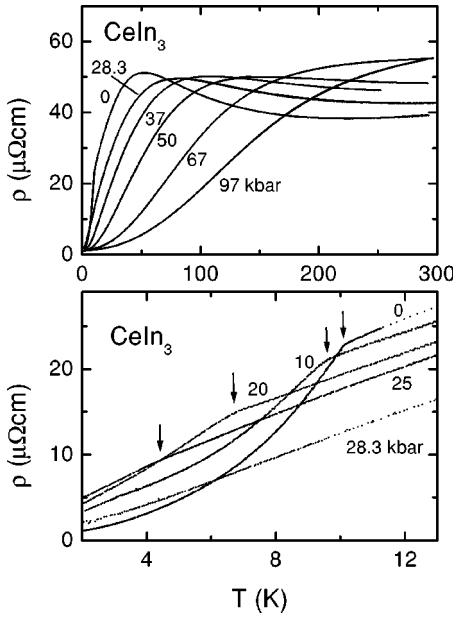


FIG. 2. Temperature dependence of the electrical resistivity $\rho(T)$ for different pressures. The lower frame shows $\rho(T)$ near the magnetic transition in detail.

known up to now for CeIn₃. However, the temperature dependence of the resistivity below T_N can be described by a power law $\Delta\rho(T) = \rho(T) - \rho_0 \propto T^n$. At ambient pressure we find $n = 2.3 \pm 0.1$. The exponent $n > 2$ reflects the magnon contribution to the resistivity. The residual resistivity is $\rho_0 = 0.5 \mu\Omega \text{ cm}$, which is very low and shows the high quality of the sample. The enhancement of the prefactor $A = 0.15 \pm 0.04 \mu\Omega \text{ cm/K}^2$ indicates the existence of heavy electrons and is consistent with the linear temperature term of the specific heat at low temperatures $C/T = 0.13 \text{ J/mol K}^2$.^{21,28,29} Assuming one electronic carrier per unit cell, this gives an effective mass at $P = 0$ of $m^* = 60m_e$. The value for $A/\gamma^2 \approx 8.9 \times 10^{-6} \mu\Omega \text{ cm (mol K/mJ)}^2$ is near the empirical universal value for heavy-fermion systems given by Kadowaki and Woods.³⁰

At low pressures $P \leq 10 \text{ kbar}$, T_M and T_N are only slightly pressure dependent. Up to 1.7 kbar T_N seems to be independent of pressure while the sublattice magnetization decreases by 4%.²⁰ The situation changes for $P \geq 15 \text{ kbar}$. Now T_M increases, the resistivity maximum broadens, and T_N decreases strongly with increasing pressure. For 28.3 kbar we find $T_M = 81 \pm 3 \text{ K}$. At the highest investigated pressures $P = 67 \text{ kbar}$ and $P = 97 \text{ kbar}$ no maximum can be observed on the bare curve, and the temperature dependencies of the resistivity are comparable to a mixed-valent system like CeNi₂Si₂, for example. The increase of T_M is consistent with the increase of the Kondo temperature T_K determined by NQR measurements.³¹ For $P > 15 \text{ kbar}$ the nuclear spin-lattice relaxation rate $1/T_1$ starts to decrease from a constant value at high temperatures. This suggests that T_K is higher than T_N for $P > 15 \text{ kbar}$ as a constant value of T_1 is characteristic of the spin dynamic of localized moments above T_K while a Korringa law is observed below T_K . A similar situation is observed in many other Kondo-lattice com-

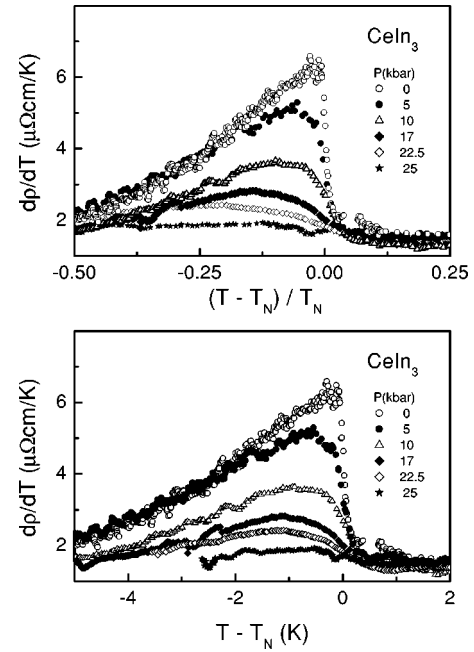


FIG. 3. Temperature dependence of the derivative of the resistivity $d\rho/dT$ for different pressures as a function of $(T - T_N)/T_N$ (upper frame), and $T - T_N$ (lower frame). A broadening of the transition is clearly seen for pressures $P > 10 \text{ kbar}$.

pounds too, both in experiments under hydrostatic pressure [e.g., CeCu₂Ge₂ (Ref. 32)] and in doping experiments [e.g., CeCu₂(Si_{1-x}Ge_x)₂,³³ Ce(Pd_{1-x}Ni_x)₂Ge₂,³⁴ or Ce(Cu_{1-x}Ni_x)₂Ge₂ (Ref. 35)]. If T_N is far below T_K the $4f$ electrons have more itinerant behavior; their sensitivity to the crystal-electric field (CEF) is strongly depressed since T_K has increased under pressure (see pressure variation of T_M). At T_N the localized character of the f electrons is lost and the heavy-fermion band clearly is established. When T_K is lower than or comparable to T_N , a description of the magnetic ordering in the frame of a Kondo lattice with pressure induced demagnetization of the Ce moment was used;²⁰ it reproduces well an initial pressure independent value of T_N coupled with a decrease of the sublattice magnetization (4% at 1.7 kbar). We will emphasize later that at high pressure ($P > 15 \text{ kbar}$) the description by spin-fluctuation theory for itinerant electrons appears valid.

For low pressures the anomaly in the resistivity at T_N is very sharp and in $d\rho(T)/dT$ we find a specific heat-like behavior, $d\rho(T)/dT \propto C_P$, as expected for a mean field-like transition.³⁶ Figure 3 shows, respectively, the temperature variation of the derivative $d\rho/dT$ of the resistivity versus a reduced $(T - T_N)/T_N$ and absolute $T - T_N$ variable. With both variables, the resistivity anomaly appears to be broad above 10 kbar. The broadening of the transition cannot be explained only by possible pressure gradients in the cell, as we observe no increase of the superconducting transition width of the Pb manometer, but is an intrinsic effect of the material. In critical phenomena,³⁷ impurities change the critical behavior only if the specific heat diverges at the critical temperature according to the Harris criterion. Here the phenomenon is quite different and more similar to surface prob-

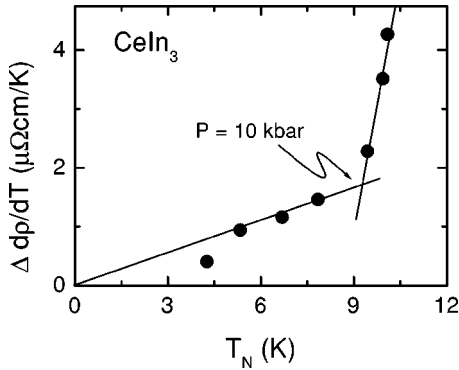


FIG. 4. Amplitude of the resistivity anomaly $\Delta(dp/dT)$ as a function of the magnetic transition temperature T_N . A clear change of regime occurs at $P=10$ kbar (lines to guide the eyes).

lems found in magnetism,³⁸ for some local structural transition,³⁹ and the appearance of localized states near defects in helicoidal transitions.⁴⁰ Here defects such as dislocations or stacking faults induce strong pressure gradients which modify the condition for the occurrence of long range magnetic order. Disorder on a microscopic scale causes magnetically ordered clusters to coexist with paramagnetic clusters in agreement with recent NQR measurements where a broadening of the lowest frequency resonance line occurs between 23.6 and 24.4 kbar.⁴²

Another experimental observation is that $d\rho/dT$ reaches a maximum near T_N . As T_N decreases the maximum value of $d\rho/dT$ also decreases, which is of course directly related to the pressure-induced decrease of the sublattice magnetization m . In spin-fluctuation theory,^{43–45} m varies like $T_N^{3/4}$. If we assume $d\rho/dT \propto m^2$, at 25 kbar we expect a decrease of the resistivity anomaly by a factor 5 in comparison to $P=0$ kbar, in qualitative agreement with Fig. 3. Another comparison can be made with the predictions given by scaling theory for the specific heat C , if it is assumed that the proportionality between C and $d\rho/dT$ is valid;^{36,46} here the amplitude of the specific heat at T_N will change from a $T_N^{3/2}$ to a linear T_N dependence as we approach the quantum critical point from the ordered antiferromagnetic phase.⁴⁷ We see in Fig. 4 a clear change of regime at $T_N=9$ K, i.e., for $P \leq 10$ kbar. It is worthwhile to underline that near P_c , Zülicke and Millis⁴¹ predict a specific heat jump $\Delta C \propto T_N^2$, whereas experimentally no such drastic decrease of $d\rho/dT$ is found. However, neutron scattering experiments to determine the sublattice magnetization m and direct specific heat measurements when T_N collapses are necessary for a sound comparison with theory. To summarize, the analysis of the resistivity anomaly reproduces well the scaling predictions despite the existence of a broadening of the anomaly near T_N for $T_N \rightarrow 0$. The striking point is that 10 kbar appears to be a cross-over pressure in the P variation of the amplitude of $d\rho/dT$ and the broadening; it corresponds to the clear entrance into the regime where T_K becomes greater than T_N (see NQR results of Ref. 31). A similar broadening of the magnetic transition and variation in the temperature dependence of the amplitude of $d\rho/dT$ with T_N has been observed in CePd_2Si_2 , as well as a change of regime also near 10 kbar.²⁵ Further

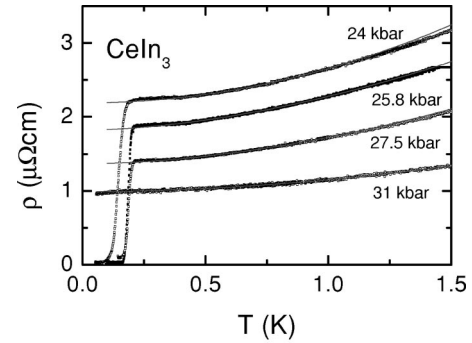


FIG. 5. Low temperature resistivity of CeIn_3 for pressures around $P_c=26.5$ kbar. A complete superconducting transition occurs. The lines are fits with a power law dependence $\rho = \rho_0 + A_n T^n$ (see the text).

investigations would require direct thermodynamic measurements as well as microscopic probes for the magnetism [value of $m(T, P)$] in the pressure range up to P_c and the identification of structural defects.

The decrease of the magnetic ordering temperature T_N can be extrapolated to $T=0$ K at the critical pressure $P_c = 26.5 \pm 1$ kbar, which is comparable to the value $P_c = 26$ kbar obtained by the Cambridge group.¹ For $P = 27.5$ kbar no anomaly due to a magnetic ordered state could be detected. In the spin-fluctuation model^{43–45} the magnetic transition temperature collapses as $(P - P_c)^{z/d}$ near the critical pressure, where z is the dynamical critical exponent and d the dimension of the system. A fit of $T_N(P)$ for $P > 10$ kbar gives an exponent of about 0.7, which is close to the expected value of $2/3$ for a three-dimensional antiferromagnetic system. However, it is difficult to determine this critical exponent, as there are not enough points near the critical pressure P_c .

In the critical region near the magnetic instability a sharp and complete superconducting transition is found between 24 and 27.5 kbar at low temperatures. The pressure range of the superconducting phase seems to be somewhat broader in the present work than in Ref. 1. This may be an intrinsic effect associated with our flux grown sample or it may be due to pressure inhomogeneities as discussed previously. In Fig. 5 we show the resistivity for pressures near P_c at temperatures below 1.5 K. The onset of the superconducting transition at 24 kbar is at $T_c = 170$ mK and the width of the transition is $\Delta T_c = 46$ mK. For 25.8 kbar we find $T_c = 198$ mK and $\Delta T_c = 24$ mK. The maximum of $T_c = 204$ mK and the sharpest transition is found for 27.5 kbar ($\Delta T_c = 20$ mK). Only a small drop of the resistivity is found for 31 kbar at $T_c = 100$ mK. These findings are in good agreement with the results obtained by the Cambridge group in a piston cylinder cell. It is interesting that the pressure range of the superconducting phase seems to be centered around P_c . The same behavior is found in CePd_2Si_2 .^{1,24,25} For each case the superconducting phase is found only in a range of $P_c \pm 4$ kbar. In CePd_2Si_2 it is remarkable that the resistive transition is often only complete at P_c . For CeIn_3 the zero field transition appears to be robust; however, in magnetic field a finite residual resistivity appears below T_c (see the following).

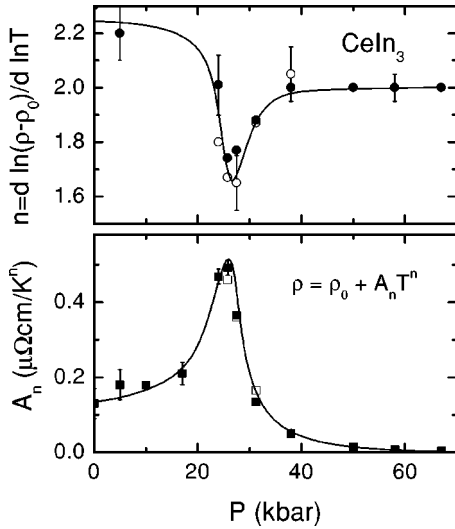


FIG. 6. Upper frame: Pressure dependence of the resistivity exponent n , closed circles correspond to fits in the temperature range $0.4 < T < 1$, open circles in an extended temperature range $T < 1.5$. Lower frame: The prefactor A_n as function of pressure; closed squares: n fixed to 2; open squares: $n \neq 2$. The lines are drawn to guide the eyes.

The normal state properties near the critical pressure show clear deviations from Fermi-liquid behavior. The resistivity can be described as a power law $\rho(T) = \rho_0 + A_n T^n$ where the exponent n and the prefactor A_n are strongly pressure dependent in the critical region (see Fig. 6 and discussion below). At low temperatures ($T < T_N$ and $T < T_I$) the situation may be clearer as one can expect $n > 2$ in the magnetic ordered phase, and $n = 2$ in the so-called Fermi-liquid, quantum disordered regime, insofar as the very-low-temperature regime $T < T_I$ can be achieved. Just at the quantum critical point as T_I collapses, n can differ from the Fermi-liquid value; for example, $n \approx 1.5$, averaging all scattering on the Fermi surface. The lines in Fig. 5 are fits of $\rho(T)$ in the temperature range between 0.4 and 1 K and give an excellent description of the data in the fitting range. It is difficult to give an exact value for the exponent n , as n is slightly temperature dependent below 1.5 K. If one calculates the local derivative $n = d \ln(\rho - \rho_0) / d \ln T$ the values for n at 1.5 K are somewhat smaller than at 500 mK. The main result of this analysis is shown in Fig. 6. A sharp minimum in $n(P)$ occurs at P_c , the full width of this minimum is 7 kbar with a steeper variation in the antiferromagnetic domain than in the paramagnetic regime. The minimum is characteristic of a QCP and observed in other systems too.^{24,25,48} In the antiferromagnetic ordered regime, we find a pressure independent value of $n = 2.2 \pm 0.1$. Here the power law dependence is only a rough parametrization for the resistivity and exponent $n > 2$ reflects the magnon contribution. For $T \rightarrow 0$ K a T^2 temperature dependence is expected in the experiment in this pressure range as well, because the magnon scattering will then be negligible in comparison with the contribution of the heavy quasiparticle. As the measurements are restricted to a finite temperature of $T \approx 50$ mK, we find this elevated value. For $P > P_c$ a Fermi-liquid behavior is recovered and $\rho(T)$ shows a

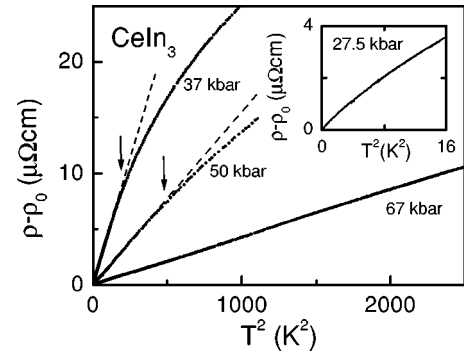


FIG. 7. Electrical resistivity $\Delta\rho = \rho - \rho_0$ as a function of T^2 for $P > P_c$. The arrows indicate the crossover temperature T_I . The inset shows $\Delta\rho$ for $P = 27.5$ kbar, here we observe no crossover to a Fermi-liquid state.

clean T^2 dependence up to a crossover temperature T_I . T_I is determined by the temperature, where deviations of 5% from a linear behavior in a $\rho(T)$ vs T^2 plot occur (see Fig. 7). For the highest pressure $P = 97$ kbar the T^2 dependence is valid up to about 90 K. The pressure dependence of T_I is shown in the phase diagram (see Fig. 1). T_I increases almost linearly with pressure as expected in the antiferromagnetic spin-fluctuation theory at two or three dimensions.⁴³⁻⁴⁵ In the critical region the exponent is noticeably lower than 2 and we find $n = 1.74$ and $n = 1.77$ for $P = 25.8$ kbar and $P = 27.5$ kbar for $T = 500$ mK. If we fit $\rho(T)$ up to 1.5 K, we get $n = 1.67$ and $n = 1.65$. The Cambridge group reports $n = 1.6 \pm 0.2$. The breakdown of the Fermi-liquid theory is expected at the QCP, the spin-fluctuation theory with no “hot spot” consideration (see the following) predicts an exponent $n = 1.5$ just at the critical pressure whereas slightly away from P_c the Fermi-liquid behavior should be recovered.

The spin-fluctuation model⁴³⁻⁴⁵ neglects the influence of the Fermi surface and of disorder scattering completely. It is expected that near the critical point the scattering is enhanced only on parts of the Fermi surface which are connected to the antiferromagnetic ordering wave vector \mathbf{Q} , but in a very clean system, the scattering processes on other parts of the Fermi surface may shortcut this scattering and a T^2 dependence should be observed at very low temperatures.⁴⁹ The recent model of Rosch⁵⁰ takes impurity scattering into account, and it was shown that it leads to an averaging of the scattering rate on all the Fermi surface and exponents $n \rightarrow 1$ are expected in real samples with a very small amount of defects, whereas $n = 1.5$ should be observed in dirty samples. Indeed, exponents $n < 1.5$ are found in the experiment for CePd₂Si₂ (Refs. 1, 24, and 51) or CeNi₂Ge₂ (Refs. 5 and 7) at the critical pressure. However, the low exponent found in these compounds which have a large magnetic anisotropy may also be the result of lower dimensional spin-fluctuations.¹ In cubic CeIn₃ the argument of a lower dimension can be excluded. The minimum of n at P_c as a function of pressure is quite sharp in CeIn₃ (see Fig. 6). The fact that the observed minimum value of n is slightly higher than 1.5 may be due to the fact that the investigated samples were not exactly at the QCP, but very near to it. A minimum value of $n \approx 1.6$ is found in all reported measurements for

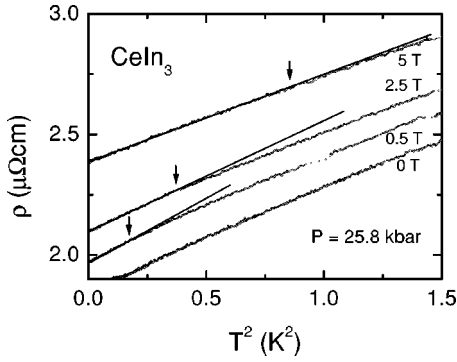


FIG. 8. Temperature dependence of the resistivity ρ vs T^2 for $P=25.8$ kbar for different magnetic fields. The arrows indicate up to which temperature $\Delta\rho \propto T^2$.

rather clean materials. This behavior is quite different from the “hot spot” model of Rosch. Measurements of the heavy fermion dynamical susceptibility show that the “hot spots” are not so well defined since a large independent wave vector contribution in the dynamical susceptibility occurs; the decomposition between “hot” and “cold spots” is thus not obvious. The observation of a deep minimum of n at P_c shows that in CeIn_3 the quantum critical point is well defined despite the broadening observed in the resistivity anomaly on approaching T_N when $P \rightarrow P_c$. The cause of the deviations from the Fermi-liquid behavior are not inhomogeneities in the material which could lead to a distribution of Kondo temperatures where the Kondo effect on each f electron sets a different temperature scale,⁵² or to the formation of a Griffith phase.⁵³ These models succeed in explaining deviations from Fermi liquid behavior in doped systems like $\text{UCu}_{1-x}\text{Pd}_x$, $\text{U}_{1-x}\text{Th}_x\text{Pd}_2\text{Al}_3$, or $\text{Y}_{1-x}\text{U}_x\text{Pd}_3$.^{54–57} At our experimental accuracy, a critical point exists and not a large critical domain.

In Fig. 6 we also show a crude estimation of the pressure dependence of the prefactor $A_2 \equiv A$. To determine the Fermi-liquid prefactor $A_2 \equiv A$, we performed fits with a fixed value $n=2$ at low temperatures. In the antiferromagnetic ordered region $P < 20$ kbar, A increases only a little in comparison to the value $A = 0.15 \mu\Omega \text{ cm K}^{-2}$ at ambient pressure. A very strong maximum appears in the critical pressure range. For $P > P_c$, A decreases very fast, $A = 1.7 \text{ n}\Omega \text{ cm K}^{-2}$ at $P = 97$ kbar. In spin-fluctuation theory it is predicted that A

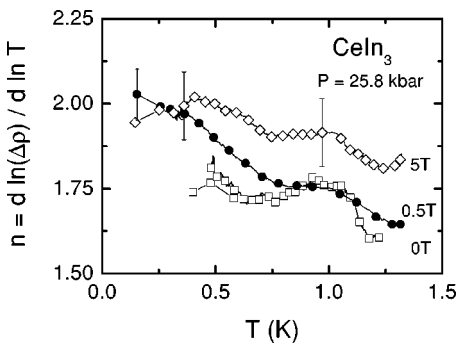


FIG. 9. Temperature dependence of the resistivity exponent n for $P=25.8$ kbar at different applied magnetic fields H .

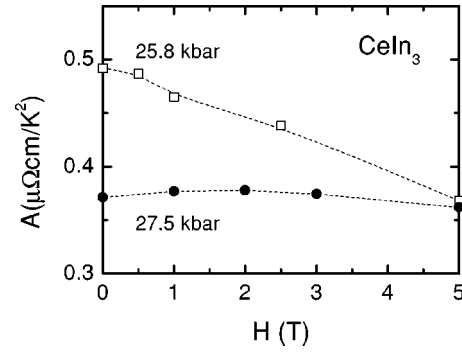


FIG. 10. Field dependence of the prefactor A of the resistivity $\Delta\rho = AT^2$ at $P=25.8$ and 27.5 kbar.

diverges as $(P - P_c)^{-1/2}$ at the critical boundary of the antiferromagnetism on the paramagnetic side,⁵⁸ while the temperature range in which the T^2 dependence is valid, decreases linearly approaching P_c . The pressure dependence of A observed here shows a faster divergence of A from the paramagnetic side like $(P - P_c)^{-1.2}$. The value of A gives an estimate of the pressure variation of the effective mass m^* assuming $m^* \propto \gamma \sqrt{A}$, which is valid far from P_c in heavy-fermion systems. We find an increase of the effective mass by a factor 2. Precisely at the critical pressure the situation is more complicated as the A coefficient is predicted to diverge but the specific heat coefficient γ remains finite for $T \rightarrow 0$ K.

In an applied external magnetic field $\rho(T)$ we expect a recovery of Fermi-liquid behavior, as the strong spin-fluctuations are suppressed as one escapes from the antiferromagnetic domain. In fact the resistivity in external field can also be modeled with a power law $\rho - \rho_0 = A_n T^n$. Figure 8 shows the resistivity for $P=25.8$ kbar vs T^2 at different external magnetic fields. In Fig. 9 we plotted the temperature dependence of the exponent n which allows a more detailed analysis. Below 1 K the temperature dependence of n for $H=0$ T is very small and n is almost constant within the error bars, but in a field $H=0.5$ T, just above the upper critical field, a Fermi-liquid behavior is found below 250 mK. It seems that at this pressure, which is just below the critical pressure at $P_c \approx 26.5$ kbar, we do not reach a T^2 dependence at zero field, because the sample becomes superconducting. The situation is comparable to CeCu_2Si_2 , where the superconducting phase is also formed out of a non-Fermi-liquid regime.³ The temperature range in which the Fermi-liquid description holds increases with increasing magnetic field, for 5 T almost up to 1 K. For $P=27.5$ kbar, the non-Fermi-liquid behavior is more robust against magnetic field, and we find an almost constant value of $n=1.8$ in the temperature regime below 1 K and for fields up to 5 T. This is analogous to the findings in CePd_2Si_2 , where at the critical pressure the Fermi-liquid behavior is not recovered in fields up to 6 T.²⁴ In Fig. 10 we plotted the field dependence of the prefactor A for $P=25.8$ and 27.5 kbar. The different behavior in the field dependence of A may reflect their location on opposite sides of P_c where one may expect a collapse of the $H-T$ magnetic phase diagram associated with a modification of the Brillouin zone. Qualitatively, on the antiferro-

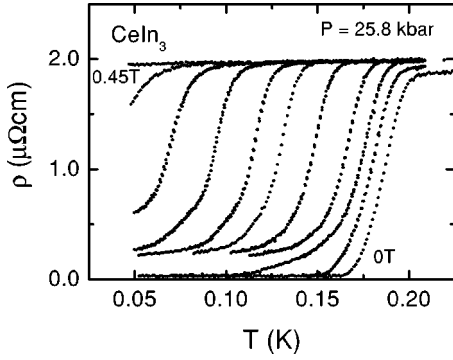


FIG. 11. Temperature dependence of the resistivity for $P = 25.8$ kbar for $H = 0, 0.04, 0.07, 0.1, 0.15, 0.2, 0.25, 0.3, 0.35, 0.4,$ and 0.45 T.

magnetic side a field sweep leads to a crossing of the magnetic phase transition and therefore a strong variation of A ; on the paramagnetic side the weak dependence of $A(H)$ indicates that any pseudometamagnetic transition like that intensively studied for the $Ce_{1-x}La_xRu_2Si_2$ series is at very high magnetic field.^{59,60} These results are a first indication on the field sensitivity of both phases. As for many heavy-fermion systems, there is a lack of basic thermodynamic studies under pressure to aid interpretation. Even at $P=0$ it is only known that the antiferromagnetic phase in the H - T phase diagram extends to very high magnetic field.^{61,62}

The analysis of the upper critical field H_{c2} can be very informative and reveals details about the pressure-induced superconducting state. We investigated H_{c2} in detail for 25.8 and 27.5 kbar. Figure 11 shows the superconducting transition for different fields up to $H=0.45$ T at $P=25.8$ kbar. The transition is complete for fields $H < 0.1$ T. For higher fields the resistivity shows an unexplained step to a constant value of 10% of the normal state resistivity. The upper part of the transition, which determines the tangent criterion, is not influenced by this incomplete transition. In Fig. 12 we have plotted the temperature dependence of H_{c2} for $P = 25.8$ kbar. H_{c2} was determined by temperature sweeps at constant field (circles); in addition we performed field sweeps at constant temperature. To determine H_{c2} the onset

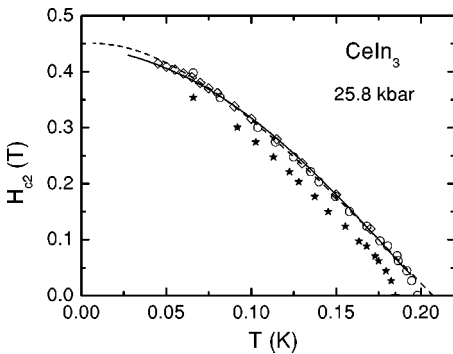


FIG. 12. Upper critical field for $P = 25.8$ kbar. Solid line is a fit within the strong coupling model with $\lambda = 1.3$, $H'_{c2} = -3.2$ T/K, and $g = 1.4$, dashed line: weak coupling in orbital limit with $H'_{c2} = -3.2$ T/K, see the text. The stars give $H_{c2}(T)$ determined by the midpoint criterion.

criterion was chosen in both cases, as the transition is no longer complete. Due to the different shape of the transition at constant field and constant temperature sweeps, H_{c2} of the field sweeps for 25.8 kbar obtained by field sweeps is slightly lower than H_{c2} of temperature sweeps and shifted by 0.04 T in Fig. 12.

In the simplest model,⁶³ clean limit and weak coupling, H_{c2} is determined by T_c , the initial slope $H'_{c2} = dH/dT|_{T=T_c}$ and the gyromagnetic ratio g of the conduction electrons. From our experimental results we find for 25.8 kbar an initial slope of $H'_{c2} = -3.2 \pm 0.2$ T/K if we neglect the strong negative curvature at low fields. However, very close to T_c the slope is poorly defined. In this model we can estimate from the slope the superconducting coherence length ξ_0 and the Fermi velocity v_F ,

$$\xi_0 = \frac{1}{0.74} \sqrt{\frac{\phi_0}{2\pi T_c H'_{c2}}}, \quad \xi_0 = 0.18 \frac{\hbar v_F}{k_B T_c}, \quad (1)$$

and verify the assumption of a clean superconductor. This yields $\xi_0 \approx 300$ Å and $v_F \approx 4500$ m/s. In any case, the superconducting coherence length is indeed much lower than the electronic mean free path, $l_e \approx 2000$ Å, which can be estimated from the residual resistivity and the coefficient of the specific heat at ambient pressure, which shows that CeIn₃ is in the clean limit. If we assume a spherical Fermi surface, we can estimate the effective mass of the electrons at the Fermi level from $m^* = \hbar k_F / v_F$, where $k_F = (3\pi^2 Z / \Omega)^{1/3}$ is the Fermi-wave vector. Z corresponds to the number of conduction electrons per unit cell and Ω is the unit cell volume in cm³. With this simplified estimation we find $m^* = 170m_0$. This value near the critical pressure is roughly three times higher than the effective mass at zero pressure calculated from the specific heat coefficient γ .

The temperature dependence of H_{c2} of CeIn₃ is shown in Fig. 12 and it is not possible to calculate $H_{c2}(T)$ in the weak coupling model consistently. The extrapolated value at $T = 0$ K, $H_{c2}(0)$ is about 0.45 T, which is close to the normal Pauli limit, $H_{c2}^P = 1.85k_B T_c = 0.36$ T assuming an electronic g value equal to 2. However, the almost linear variation of $H_{c2}(T)$ between 60 and 170 mK is inconsistent with a strong Pauli limitation and in fact resembles a purely orbital limited H_{c2} . As shown in Fig. 12 the data can be well described by an orbital limited $H_{c2}^{orb} = H_{c2}(0) \approx 0.45$ T = $-0.693H'_{c2}T_c$ weak coupling model with the exception of the points close to T_c . However, this fit is obtained with different calculated value of T_c ($T_c^{calc} = 0.207$ K) to those found experimentally and a slope of $H'_{c2} = -3.2$ T/K, i.e., neglecting the initial curvature. The absence of Pauli limitation is somewhat surprising so we further tried to calculate $H_{c2}(T)$ in a strong coupling limit, since it will increase the Pauli limit (a factor $\sqrt{\lambda}$ for $\lambda \rightarrow \infty$). Details of the model used are given in Ref. 64. In this calculation three parameters must be chosen, the coupling strength λ , the gyromagnetic ratio g , which restricts the Pauli limit, and the initial slope H'_{c2} at T_c . Different g factors can be tuned. If the crystal field effect (CEF) is well resolved, i.e., the low temperature Kondo temperature is weaker than the CEF, $g = 1.4$ for the lowest crystal field

level. However for $P \sim P_c$, the localized character of the f electron may be lost so the g value is questionable. The dashed line in Fig. 12 is a calculation with $g = 1.4$, $\lambda = 1.3$, and an initial slope -3.2 T/K given by orbital limitation. The coupling λ is linked to mass renormalization: $\lambda = m_{fl}^*/m_b^* - 1$ where m_b^* is the band mass of the heavy quasiparticle and m_{fl}^* takes into account in addition the spin-fluctuation effects. The λ value points to an enhancement of the effective mass of $m_{fl}^*/m_b^* \approx 2.3$. The Fermi surface of CeIn₃ at $P=0$ has been partly determined by de Haas-van Alphen oscillations.^{61,62} Up to now a comparison with the average effective mass $m^* = 60$ measured by specific heat is not possible. Furthermore the new magnetic Brillouin zone below T_N becomes centered cubic with half the volume of the simple paramagnetic Brillouin zone. At $P=0$ the highest detected mass is $21 m_0$. From the plot of H_{c2} over a large field range (i.e., neglecting the initial curvature) an average mass of 170 is found at P_c . From the P dependence of A one suspects a mass enhancement of a factor 2 from the $P=0$ value. A similar rather low value of λ is obtained for CePd₂Si₂ and CeCu₂Si₂ near their QCP.^{13,24,65} By contrast to UBe₁₃ where large strong coupling effects are reported the situation is quite opposite as here for CeIn₃, where the effective bandwidth T_K is higher than T_c . In UBe₁₃, the damping rate of the quasiparticle with energy of the order of $k_B T_c$ is comparable to T_c itself, which leads to the strong coupling analysis in H_{c2} .^{66,67} Of course here the rather weak value of λ is consistent with the moderate effective mass enhancement at P_c given by antiferromagnetic spin fluctuations. That supports a coherent picture for the establishment of superconductivity via the spin-fluctuation mechanism. However a full comparison now needs realistic theoretical calculations with an unconventional order parameter (d or p) and not with the s wave model presently used. Up to now analyses have been done only at $H=0$ and in the case of quasi-two-dimensional systems.⁶⁸⁻⁷⁰

To calculate H_{c2} for low fields $H < 0.05T$ in CeIn₃, we may have to take into account that the effective mass m_{fl}^* may be not constant in a magnetic field, but probably strongly reduced. This indicates that the coupling constant λ is field dependent and decreases rapidly in field due to the suppression of the spin-fluctuation effects. However no drastic initial field decrease of A is observed, especially in the field range where superconductivity exists. Experimentally, it is necessary now to investigate the upper critical field at small fields in more detail and extend the studies of H_{c2} in pressure range. Of course, we need also to verify that the initial nonlinearity of H_{c2} with temperature is an intrinsic effect or not. If it is intrinsic m^* will be field dependent and thus our explanation through A quite qualitative.

Previous analysis of $H_{c2}(T)$ on Pauli paramagnetic superconductors with large mass enhancement^{71,72} have been achieved for arbitrary electronic mean free paths using the fact that the orbital upper critical field may be enhanced by unknown mechanism; a relation has been made with magnetoresistive effects in the normal state above T_c . We emphasize that CeIn₃ is clearly a clean superconductor, i.e., $\xi_0 \ll l_e$ and therefore provides a good opportunity to analyze the upper critical field with simple models.

IV. CONCLUSION

In this work we have studied the phase diagram of CeIn₃ under pressure up to 100 kbar by resistivity measurements. The samples investigated are grown out of excess In. In the vicinity of the critical pressure $P_c \approx 26.5$ kbar, we confirmed the existence of a superconducting phase below 0.2 K. The very good agreement with earlier work on samples grown in a different way and by using different pressure techniques shows that this very interesting phase diagram is robust and reproducible. At low pressures the antiferromagnetic transition has a mean field-like anomaly in the resistivity. On reaching the critical pressure, the magnetic transition broadens significantly. This is not due to pressure inhomogeneities but to an effect of the material, and is related to the hierarchy between the magnetic correlation length, the superconducting coherence length, and the electronic mean free path. However, the temperature dependence of $\rho(T)$ on both sides of P_c at very low temperature shows that the quantum critical point is well defined and there is no critical domain. The normal state properties show in the critical pressure range deviations from Fermi-liquid behavior. Below the critical pressure a T^2 dependence of the resistivity is recovered in magnetic fields just above the upper critical field, whereas just above P_c the non-Fermi-liquid temperature dependence is more robust against external fields. A T^2 dependence is restored in the paramagnetic regime of the phase diagram and the crossover temperature T_I increases linearly with pressure. The temperature dependence of the upper critical field $H_{c2}(T)$ can be analyzed with a strong coupling model and supports strongly a spin-fluctuation mechanism.

ACKNOWLEDGMENTS

We thank J.-P. Brison and D. Jaccard for many fruitful discussions. One of us (G.K.) acknowledges the ESF within the FERLIN program and the EC (MCFI-1999-00474) for financial support. P.C.C. wishes to acknowledge CEA Grenoble for support. In addition this work was supported by the Director of Energy Research, Office of Basic Energy Sciences under Contract No. W-7405-Eng-82.

*On leave in CEA Grenoble. Permanent address: Department of Physics and Astronomy and Ames Laboratory, Iowa State University, Ames, IA 50011.

¹N.D. Mathur, F.M. Grosche, S.R. Julian, I.R. Walker, D.M. Freye, R.K.W. Haselwimmer, and G.G. Lonzarich, *Nature* (London) **394**, 39 (1998).

²F. Steglich, J. Aarts, C.D. Bredl, W. Lieke, D. Meschede, W. Franz, and H. Schäfer, *Phys. Rev. Lett.* **43**, 1892 (1979).

³P. Gegenwart, C. Langhammer, C. Geibel, R. Helfrich, M. Lang, G. Sparn, F. Steglich, R. Horn, L. Donnevert, A. Link, and W. Assmus, *Phys. Rev. Lett.* **81**, 1501 (1998).

⁴S.J.S. Lister, F.M. Grosche, F.V. Carter, R.K.W. Haselwimmer,

- S.S. Saxena, N.D. Mathur, S.R. Julian, and G.G. Lonzarich, *Z. Phys. B: Condens. Matter* **103**, 263 (1997).
- ⁵P. Gegenwart, F. Kromer, M. Lang, G. Sparn, C. Geibel, and F. Steglich, *Phys. Rev. Lett.* **82**, 1293 (1999).
- ⁶D. Braithwaite, T. Fukuhara, A. Demuer, I. Sheikine, S. Kambe, J.-P. Brison, K. Maezawa, T. Naka, and J. Flouquet, *J. Phys.: Condens. Matter* **12**, 1339 (2000).
- ⁷F.M. Grosche, P. Agarwal, S.R. Julian, N.J. Wilson, R.K.W. Haselwimmer, S.J.S. Lister, N.D. Mathur, F.V. Carter, S.S. Saxena, and G.G. Lonzarich, *J. Phys.: Condens. Matter* **12**, L533 (2000).
- ⁸C. Petrovic, P.G. Pagliuso, M.F. Hundley, R. Moshovich, J.L. Sarrao, J.D. Thompson, and Z. Fisk, *Nature (London)* (unpublished); J.D. Thompson, R. Moshovich, N.J. Curro, P.C. Hammel, M.F. Hundley, M. Jaime, P.G. Pagliuso, J.L. Sarrao, C. Petrovic, Z. Fisk, F. Bouquet, R.A. Fisher, and N.E. Phillips, *J. Magn. Magn. Mater.* (unpublished).
- ⁹D. Jaccard, K. Behnia, and J. Sierro, *Phys. Lett. A* **163**, 475 (1992).
- ¹⁰R. Movshovich, T. Graf, D. Mandrus, J.D. Thompson, J.L. Smith, and Z. Fisk, *Phys. Rev. B* **53**, 8241 (1996).
- ¹¹F.M. Grosche, S.R. Julian, N.D. Mathur, and G.G. Lonzarich, *Physica B* **223&224**, 50 (1996).
- ¹²S. Raymond, D. Jaccard, H. Wilhelm, and R. Cerny, *Solid State Commun.* **112**, 617 (1999).
- ¹³S. Raymond and D. Jaccard, *Phys. Rev. B* **61**, 8679 (2000).
- ¹⁴I.R. Walker, F.M. Grosche, D.M. Freye, and G.G. Lonzarich, *Physica C* **282-287**, 303 (1997).
- ¹⁵H. Hegger, C. Petrovic, E.G. Moshopoulou, M.F. Hundley, J.L. Sarrao, Z. Fisk, and J.D. Thompson, *Phys. Rev. Lett.* **84**, 4986 (2000).
- ¹⁶J.M. Lawrence and S.M. Shapiro, *Phys. Rev. B* **22**, 4379 (1980).
- ¹⁷A. Benoit, J.X. Boucherle, P. Convert, J. Flouquet, J. Pellau, and J. Schweizer, *Solid State Commun.* **34**, 293 (1980).
- ¹⁸W. Groß, K. Knorr, A.P. Murani, and K.H.J. Buschow, *Z. Phys. B* **37**, 123 (1980).
- ¹⁹A.P. Murani, A.D. Taylor, R. Osborn, and Z.A. Bowden, *Phys. Rev. B* **48**, 10 606 (1993).
- ²⁰L.E. DeLong, R.P. Guertin, and S. Foner, *Solid State Commun.* **32**, 833 (1979).
- ²¹P. Morin, C. Vettier, J. Flouquet, M. Konczykowski, Y. Lassailly, J. Mignot, and U. Welp, *J. Low Temp. Phys.* **70**, 377 (1988).
- ²²J. Flouquet, P. Haen, P. Lejay, P. Morin, D. Jaccard, J. Schweizer, C. Vettier, R.A. Fisher, and N.E. Phillips, *J. Magn. Magn. Mater.* **90&91**, 377 (1990).
- ²³P.C. Canfield and Z. Fisk, *Philos. Mag. B* **65**, 1117 (1992).
- ²⁴I. Sheikin, D. Braithwaite, J.-P. Brison, S. Raymond, D. Jaccard, and J. Flouquet, *J. Low Temp. Phys.* **122**, 591 (2001).
- ²⁵A. Demuer, Ph.D. thesis, University of Grenoble, 2000; A. Demuer, I. Sheikin, D. Braithwaite, B. Fåk, A. Huxley, S. Raymond, and J. Flouquet, *J. Magn. Magn. Mater.* (to be published).
- ²⁶B. Cornut and B. Coqblin, *Phys. Rev. B* **5**, 4541 (1972); Y. Lassailly, A.K. Bhattacharjee, and B. Coqblin, *ibid.* **31**, 7424 (1985).
- ²⁷Y. Lassailly, S.K. Burke, and J. Flouquet, *J. Phys. C* **18**, 5737 (1985).
- ²⁸S. Nasu, A.M. Van Diepen, H.H. Neumann, and R.S. Craig, *J. Phys. Chem. Solids* **32**, 2773 (1971).
- ²⁹J. Peyrard, Ph.D. thesis, University of Grenoble, 1980.
- ³⁰K. Kadowaki and S.B. Woods, *Solid State Commun.* **58**, 507 (1986).
- ³¹C. Thessieu, K. Ishida, S. Kawasaki, T. Mito, Y. Kawasaki, G.-Q. Zheng, Y. Kitaoka, and Y. Onuki, *Physica B* **281&282**, 9 (2000).
- ³²D. Jaccard, H. Wilhelm, K. Alami-Yadri, and E. Vargoz, *Physica B* **259-261**, 1 (1999).
- ³³G. Knebel, C. Eggert, D. Engelmann, R. Viana, A. Krimmel, M. Dressel, and A. Loidl, *Phys. Rev. B* **53**, 11 586 (1996).
- ³⁴G. Knebel, M. Brando, J. Hemberger, M. Nicklas, W. Trinkl, and A. Loidl, *Phys. Rev. B* **59**, 12 390 (1999).
- ³⁵N. Büttgen, R. Böhmer, A. Krimmel, and A. Loidl, *Phys. Rev. B* **53**, 5557 (1996).
- ³⁶S. Alexander, J.S. Helman, and I. Balberg, *Phys. Rev. B* **13**, 304 (1976).
- ³⁷V.S. Dotsenko, *Phys. Usp.* **38**, 347 (1995).
- ³⁸M.I. Kaganov and A.N. Omel'yanchuk, *Sov. Phys. JETP* **34**, 895 (1972).
- ³⁹A.P. Levanyuk, V.V. Osipov, A.S. Sigov, and A.A. Sobyenin, *Sov. Phys. JETP* **49**, 176 (1979).
- ⁴⁰A. Buzdin and Y. Meurdesoif, *JETP Lett.* **65**, 814 (1997).
- ⁴¹U. Zülicke and A.J. Millis, *Phys. Rev. B* **51**, 8996 (1995).
- ⁴²Y. Kohori (private communication).
- ⁴³A.J. Millis, *Phys. Rev. B* **48**, 7183 (1993).
- ⁴⁴T. Moriya and T. Takimoto, *J. Phys. Soc. Jpn.* **64**, 960 (1998).
- ⁴⁵G.G. Lonzarich, *Electron*, edited by M. Springford (Cambridge University Press, Cambridge, 1997).
- ⁴⁶M.E. Fisher and J.S. Langer, *Phys. Rev. Lett.* **20**, 665 (1968).
- ⁴⁷M.A. Continentino, *Z. Phys. B: Condens. Matter* **101**, 197 (1996); *Phys. Rev. B* **57**, 5966 (1998).
- ⁴⁸H. Wilhelm, K. Alami-Yadri, B. Revaz, and D. Jaccard, *Phys. Rev. B* **59**, 3651 (1999).
- ⁴⁹R. Hlubina and T.M. Rice, *Phys. Rev. B* **51**, 9253 (1995).
- ⁵⁰A. Rosch, *Phys. Rev. Lett.* **82**, 4280 (1999); *Phys. Rev. B* **62**, 4945 (2000).
- ⁵¹S.R. Julian, C. Pfleiderer, F.M. Grosche, N.D. Mathur, G.J. McMullan, A.J. Diver, I.R. Walker, and G.G. Lonzarich, *J. Phys.: Condens. Matter* **8**, 9675 (1996).
- ⁵²E. Miranda, V. Dobrosavljević, and G. Kotliar, *J. Phys.: Condens. Matter* **8**, 9871 (1998).
- ⁵³A.H. Castro Neto, G.E. Castilla, and B.A. Jones, *Phys. Rev. Lett.* **81**, 3531 (1998).
- ⁵⁴O.O. Bernal, D.E. Mac Laughlin, H.G. Lukefahr, and B. Andraka, *Phys. Rev. Lett.* **75**, 2023 (1995); O.O. Bernal, D.E. Mac Laughlin, A. Amato, R. Feyerherm, F.N. Gygax, A. Schenck, R.H. Heffner, L.P. Le, G.J. Nieuwenhuys, B. Andraka, H.v. Löhneysen, O. Stockert, and H.R. Ott, *Phys. Rev. B* **54**, 13 000 (1996).
- ⁵⁵M.C. de Andrade, R. Chau, R.P. Dickey, N.R. Dilley, E.J. Freeman, D.A. Gajewski, M.B. Maple, R. Moshovich, A.H. Castro Neto, G.E. Castilla, and B.A. Jones, *Phys. Rev. Lett.* **81**, 5620 (1998).
- ⁵⁶R.P. Dickey, A. Amann, E.J. Freeman, M.C. de Andrade, and M.B. Maple, *Phys. Rev. B* **62**, 3979 (2000).
- ⁵⁷D.A. Gajewski, R. Chau, and M.B. Maple, *Phys. Rev. B* **62**, 5496 (2000).
- ⁵⁸K. Ueda, *J. Phys. Soc. Jpn.* **43**, 1497 (1977).
- ⁵⁹J. Flouquet, S. Kambe, L.P. Regnault, P. Haen, J.P. Brison, F. Lapierre, and J.P. Lejay, *Physica B* **215**, 77 (1995).
- ⁶⁰P. Haen, F. Lapierre, J. Voiron, and J. Flouquet, *J. Phys. Soc. Jpn. Suppl. B* **65**, 27 (1996).

- ⁶¹K. Satoh, I. Umehara, N. Nagai, Y. Ōnuki, I. Sakamoto, M. Hunt, P. Meeson, P.-A. Probst, and M. Springford, *J. Magn. Magn. Mater.* **104-107**, 1411 (1992).
- ⁶²Y. Ōnuki and A. Hasegawa, in *Handbook on the Physics and Chemistry of Rare Earth* (Elsevier Science, Amsterdam, 1995), Vol. 20, pp. 1–103.
- ⁶³N.R. Werthammer, E. Hefland, and P.C. Hohenberg, *Phys. Rev.* **147**, 295 (1966); L.N. Bulaevskii, O.V. Dolgov, and M.O. Ptitsyn, *Phys. Rev. B* **38**, 11 290 (1988).
- ⁶⁴F. Thomas, B. Wand, T. Lühmann, P. Gegenwart, G.R. Stewart, F. Steglich, J.-P. Brison, A.I. Buzdin, L. Glémot, and J. Flouquet, *J. Low Temp. Phys.* **102**, 117 (1996).
- ⁶⁵I. Sheikin, D. Braithwaite, J.P. Brison, A.I. Buzdin, and W. Assmus, *J. Phys.: Condens. Matter* **10**, L749 (1998).
- ⁶⁶L. Glémot, J.-P. Brison, J. Flouquet, A.I. Buzdin, I. Sheikin, D. Jaccard, C. Thessieu, and F. Thomas, *Phys. Rev. Lett.* **82**, 169 (1999).
- ⁶⁷K. Hori and K. Miyake, *J. Phys. Soc. Jpn.* (unpublished).
- ⁶⁸P. Monthoux and G.G. Lonzarich, *Phys. Rev. B* **59**, 14 598 (1999).
- ⁶⁹T. Moriya and K. Ueda, *Adv. Phys.* **49**, 555 (2000).
- ⁷⁰P. Monthoux and G.G. Lonzarich, *Phys. Rev. B* **63**, 054529 (2001).
- ⁷¹L.E. DeLong, G.W. Crabtree, L.N. Hall, D.G. Hinks, W.K. Kwok, and S.K. Malik, *Phys. Rev. B* **36**, 7155 (1987).
- ⁷²L.E. DeLong, L.N. Hall, S.K. Malik, G.W. Crabtree, W.K. Kwok, and K.A. Gschneider, Jr., *J. Magn. Magn. Mater.* **63-64**, 478 (1987).